

# NEW SPATIAL-TEMPORAL PATTERNS AND THE FIRST PROGRAMMABLE ON-CHIP BIFURCATION TEST-BED

ISTVÁN PETRÁS<sup>1</sup>, TAMÁS ROSKA<sup>1,2</sup>, LEON O. CHUA<sup>2</sup>

<sup>1</sup> *Analogical and Neural Computing Laboratory, Computer and Automation Research Institute, Hungarian Academy of Sciences, Kende u.11, Budapest, 1111 - Hungary*  
petras@sztaki.hu, roska@sztaki.hu, <http://lab.analogic.sztaki.hu/index.html>

<sup>2</sup> *Electronics Research Laboratory, College of Engineering, University of California at Berkeley, Berkeley, CA 94720, USA*

In this paper we introduce a new experimental tool, a real-time programmable, spatial-temporal bifurcation test-bed. We present the experimental analysis of an antisymmetric template class. This class produces novel spatial-temporal patterns that have complex dynamics. The character of these propagating patterns depends on the self-feedback and on the sign of the coupling below the self-feedback template element. We also show how to use these patterns for morphological detection.

## 1 Introduction

Numerical simulations of spatial-temporal chaotic systems require huge digital computing power, but still that is the usual analysis tool because it offers the advantage of easy experimentation via programming. Till now, the physically implemented chaotic circuits were “hard-coded”. The new analogic cellular computing paradigm [5] places the spatial-temporal dynamics into array computer architecture. Using the new ACE4K test-bed [1] it is possible for the first time to make programmable real-time experiments and uncover new complex dynamic behaviors in the Cellular Nonlinear Network [2–6].



**Fig. 1.** Typical pattern classes. (a) The input and initial state, (b) snapshot of the output when the extra coupling is greater than zero, (c) snapshot of the output when the extra coupling is less than zero (*Chip measurements*)

The qualitative theory of nonsymmetrical feedback (*A*) templates had been first exposed in [14]. Later, several papers have studied the operation of the CNN with nonsymmetric or sign-antisymmetric templates [7–9]. They described some necessary conditions under which propagation effects occur or the solution is periodic. Other works investigated the pattern formation properties of the CNN [10] or studied the complex behavior [11–13] of the CNN. However, only a few works dealt with the case when there is a constant input. With constant input, we are able to localize the propagation effect into a certain region according to the extent of the input pattern. By using a constant input as a seed, different shapes can be generated depending on the properties of the template [15]. In the following we present an experimental analysis of a simple antisymmetric template in that case when we add only one extra coupling below the central element. We will introduce the basic template class and show how the behavior of the CNN changes from stable to chaotic states at different values of that coupling. Figure 1 shows two basic pattern classes that are generated by two different values of the key template element (the extra coupling is greater or less than zero). Throughout this paper, in the images *black color* means “+1” and *white color* means “-1”.

## 2 The Programmable CNN Model

Throughout this analysis we will only consider CNNs with *space invariant* templates. In the model, (Equation 1) we have a nonzero input  $u$  that adds a constant value to each cell. This model is implemented as the main elementary instruction of the ACE4k chip, an implementation of the CNN Universal Machine (CNN-UM) [5] architecture. Its stored programmability, via software makes it a new and ideal tool for us, as a test bed.

*Simulation.* The mathematical model of the simulation of the basic CNN dynamics is the following:

$$\dot{x}_{ij}(t) = -g(x_{ij}(t)) + \sum_{kl \in S_r} A_{kl} x_{ij,kl}(t) + \sum_{kl \in S_r} B_{kl} u_{kl} + z. \quad (1)$$

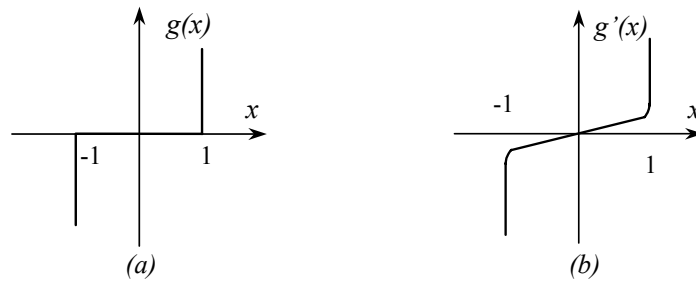


Fig. 2. (a) Hard nonlinearity  $g(\cdot)$ , (b) "Less hard" nonlinearity  $g'(\cdot)$ .

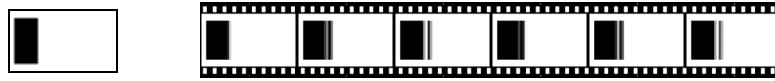
We use a so-called full range model [6]. In Equation 1,  $x_{i,j}$  denotes the state,  $A_{k,l}$  is the feedback template matrix,  $B_{k,l}$  is the control template matrix, that describes the effect of the constant input  $u_{k,l}$ , and  $z$  is the offset or bias. The integration method throughout the simulation was an *implicit Euler method*. In all cases the boundary cells are constant, except if explicitly noted differently.

*Programmable chip measurements – the experimental test bed.* The chip experiments had been made on the new ACE4k test bed. On the chip, the ideal nonlinearity (Fig. 2a) is approximated by a "less hard" nonlinearity (Fig. 2b). When the state variable  $x_{ij}(t)$  reaches the saturation limits ( $+1$ ,  $-1$ ), the  $g'(x)$  term works against the increase or decrease and keeps the value of the state within the limits.

## 3 Effect of a vertical coupling

In the following we will show how extra coupling added to a vertically uncoupled template changes the behavior of the system. At first let us consider the following one-dimensional "CCD-like" template of which solution is periodic (see Fig. 3).

$$\text{Template 1: } \mathbf{A} = \begin{bmatrix} 0 & 0 & 0 \\ 0.6 & 0.3 & -0.6 \\ 0 & 0 & 0 \end{bmatrix} \quad \mathbf{B} = \begin{bmatrix} 0 & 0 & 0 \\ 0 & 1.1 & 0 \\ 0 & 0 & 0 \end{bmatrix} \quad z = 0.1$$



**Fig. 3.** The input & initial state and the time evolution for Template 1 and snapshots of the state. Observe that the propagation decays *spatially* after a few pixels, but the oscillation remains. The initial state is the same as the input. (Simulated results)

During the time transient, cells along the right hand side border of the constant input pattern act like oscillators. The oscillators are only coupled horizontally and the rows operate independently. The oscillation propagates to the right along the row starting from the triggering constant input (black pixels), and depending on the template values, it stops (dies) after a certain distance or endures until the edge of the array.

Template 2 shows the general form of the nonsymmetrical template with an added vertical coupling. In the following we consider the  $s = -q$  case. By introducing an extra element  $r$  below of the central one, the homogeneous propagation and oscillation disappears. We get some structured pattern. The character of the structure depends on the sign of the extra template element  $r$ . (See Fig. 1)

$$\text{Template 2} \quad \mathbf{A} = \begin{bmatrix} 0 & 0 & 0 \\ s & p & q \\ 0 & r & 0 \end{bmatrix} \quad \mathbf{B} = \begin{bmatrix} 0 & 0 & 0 \\ 0 & b & 0 \\ 0 & 0 & 0 \end{bmatrix} \quad z = \xi$$

### 3.1 Positive vertical coupling ( $r > 0$ )

If the value is positive, a solid pattern is formed, however its right border is oscillating. At the beginning, the input pattern propagates oscillating to the right until a certain extent, and then the global propagation stops but cells along the right border continue oscillating (at certain parameter setting the left border can also oscillate but not propagates). Typical snapshot of the pattern is shown in Fig 1b. The ruffles along the right border of the pattern move up and right during the evolution – it is a periodic solution in time and space (See Fig. 4, corresponding template is Template 3). The exact values of the chip templates are slightly different from the template of the simulation, however the phenomenon can be reproduced quite well.

$$\text{Template 3:} \quad \mathbf{A} = \begin{bmatrix} 0 & 0 & 0 \\ 0.55 & 0.3 & -0.55 \\ 0 & 0.5 & 0 \end{bmatrix} \quad \mathbf{B} = \begin{bmatrix} 0 & 0 & 0 \\ 0 & 1.2 & 0 \\ 0 & 0 & 0 \end{bmatrix} \quad \xi = 0.6$$



**Fig. 4.** The input & initial state and the time evolution of the pattern when  $p$  is positive. Snapshots of the state (simulated results). The last snapshot shows the largest spatial extent of the generated pattern. There is no global propagation after this moment, only the ruffles travel along the right border of the pattern.

Generally, there is no oscillation inside of the structure, only along its border. These local oscillations together form the main pattern that looks like the cross-section of waves on the surface of the water (see Fig. 4).

### 3.2 Negative vertical coupling ( $r < 0$ )

When the vertical coupling is negative a texture-like oscillating pattern is formed. This pattern has a unique structure. It consists of propagating horizontal line segments that spread to the right (See Fig. 5, corresponding template is Template 4). The spatial extent

of the propagation to the right direction changes as we change the parameters but the main characteristics remain the same. Typical snapshot is shown in Fig 1c.

Let us define the bottommost row of the input pattern (black pixels) as the “first” row. The template produces a straight line for this row over a large domain of parameters values. The cells in this row are stable (saturated black pixels). The straight line serves as a constant driving for the cells in the next – “second” – row upward. The “second” row does not produce propagating pattern. Instead, we find a few neighboring oscillating cells. The third row also gives rise to periodic signal but with a different waveform and propagating pattern.

$$\text{Template 4: } \mathbf{A} = \begin{bmatrix} 0 & 0 & 0 \\ 0.9 & 0.4 & -0.9 \\ 0 & -0.5 & 0 \end{bmatrix} \quad \mathbf{B} = \begin{bmatrix} 0 & 0 & 0 \\ 0 & 1.3 & 0 \\ 0 & 0 & 0 \end{bmatrix} \quad \zeta = 2$$



**Fig. 5.** The input & initial state and the time evolution of the pattern when  $r$  is negative. Snapshots of the state (simulated).

#### 4 The effect of the central template element

If we increase the central element (self feedback) then the generated pattern gets more and more irregular and it can become chaotic. Fig. 6 shows the different dynamic regions of the system parameterized by  $r$  and  $p$  of Template 5.

$$\text{Template 5: } \mathbf{A} = \begin{bmatrix} 0 & 0 & 0 \\ 1.1 & p & -1.1 \\ 0 & r & 0 \end{bmatrix} \quad \mathbf{B} = \begin{bmatrix} 0 & 0 & 0 \\ 0 & 1.2 & 0 \\ 0 & 0 & 0 \end{bmatrix} \quad z = 0.1$$

##### Stable region

Around the periodic and chaotic region there is a stable region with various stable patterns. When  $p$  is high the effect of the input becomes dominant and therefore the output is almost the same as the input. When  $p$  is low (negative) the character of the system is diffusive. Between the two extreme values of  $p$  is a region where the effect of the input is less significant. Therefore the patterns are dominantly one-dimensional or there is no pattern at all.

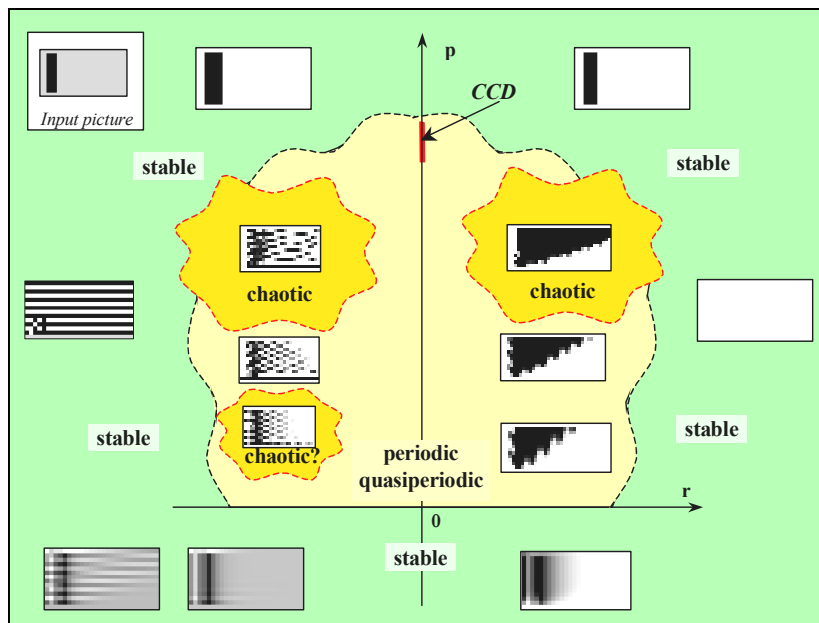
##### Periodic region

The patterns propagate periodically and they have the form of *solid wave-like* and *texture*, as it is described previously in Section 3.

##### Chaotic region

If  $p$  is large enough, the system can become chaotic. However, chaotic behavior may occur at smaller  $p$ , when  $r$  is less than zero. The reason for this can be that the constant line (the first row) becomes oscillating (See Fig. 6).

As it can be seen from the results, there is a correlation between the time evolution of the selected cells of the CNN and the dynamic behavior of the whole array. The propagation preserves the history of the dynamics, therefore the output picture can be suitable for characterizing the system without cell data measurements.



**Fig. 6.** Partitioning of the  $r$ - $p$  parameter space. The input & initial state is shown in the upper left corner. It is a three-pixel wide bar. The pictures in the different regions show few typical snapshots of outputs belonging to that region. Parameter  $p$  and  $r$  are in the  $[-2..2]$  region.

## 5 The effect of the constant input and initial state

An inherent property of the chaotic systems is the extreme sensitivity to the initial condition. In this section some results are presented related to this aspect.

*Periodic-chaotic transition.* Table 1 shows the effect of the different input patterns. The applied templates are the same for the two different inputs, i.e. the different behavior of the system is due to the difference of the input pattern. The first input is a black, five pixel wide vertical bar (periodic behavior) and the other input is a black, three pixel wide vertical bar (chaotic behavior). The input and the initial state are the same. The result shows that if the input is the five pixel wide bar then the transient of the cell is periodic. But if the input is a three pixel wide bar, the transient – and the propagating pattern too – is chaotic.

The reason for the difference is that the local oscillators along the left and right border of the bar can influence each other. This can happen only if there is no stable (saturated) vertical column of cells along the center of the bar. If the input is the three pixel wide bar there is no column of saturated ( $+I$ ) stable cells in the bar. In the other case there is horizontally at least one pixel wide column of saturated stable cells. Thus, the oscillators along the left and right border of the bar are uncoupled. The cells were sampled in the second row.

*Stable-periodic transition.* Table 2 illustrates that a single pixel perturbation can alter the general dynamic behavior of the system. The only difference between the two inputs, which are also the initial state, is that a single pixel is changed from black to gray in the middle of the right vertical edge of the bar. In the first case there is no propagation and no pattern. The second input however produces a periodic pattern. The boundary condition is periodic.

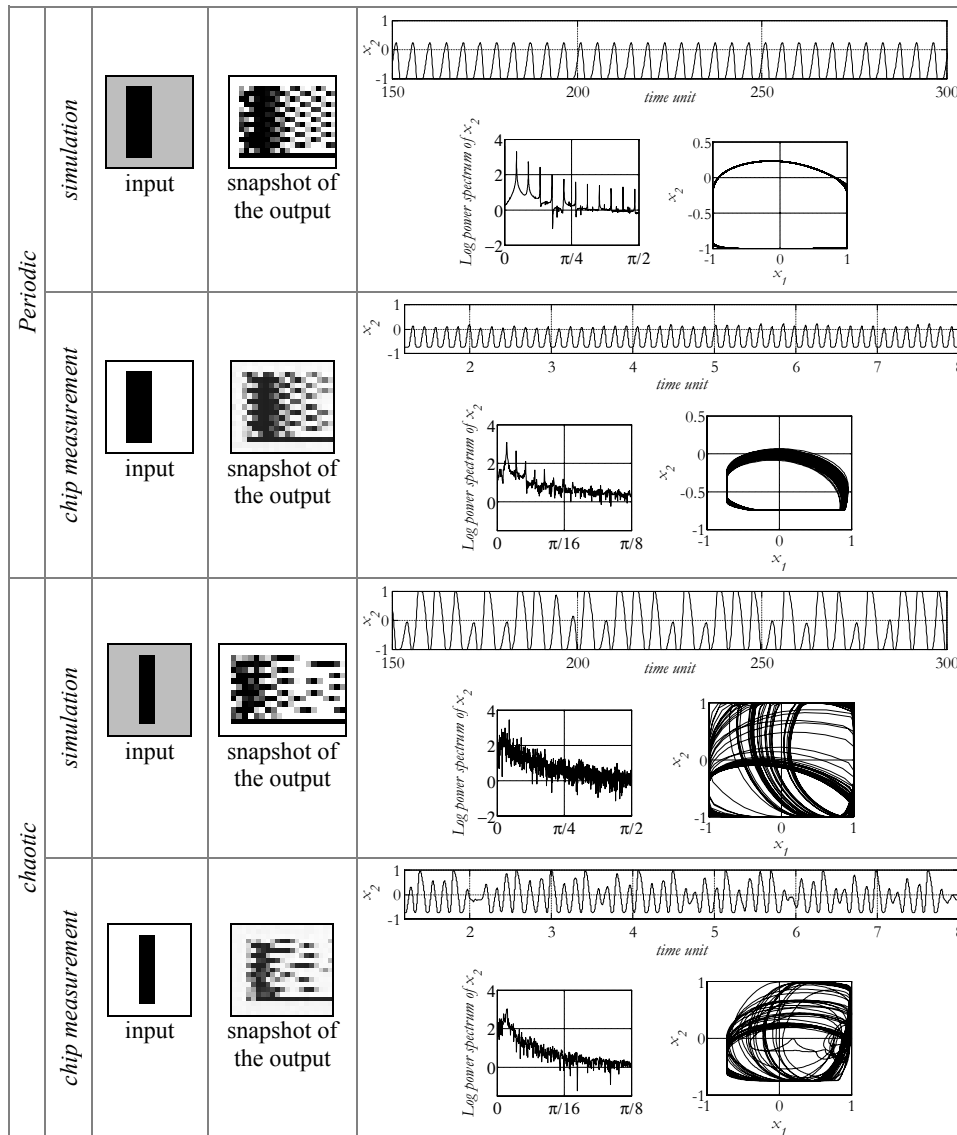
**Template 6: Template for the simulation**

**Template 7: Template for the chip measurement**


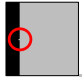

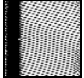
$$\mathbf{A} = \begin{bmatrix} 0 & 0 & 0 \\ 1.1 & 0.7 & -1.1 \\ 0 & -0.3 & 0 \end{bmatrix} \quad \mathbf{B} = \begin{bmatrix} 0 & 0 & 0 \\ 0 & 1.2 & 0 \\ 0 & 0 & 0 \end{bmatrix} \quad \xi = 0.1$$

$$\mathbf{A} = \begin{bmatrix} 0 & 0 & 0 \\ 0.9 & 0.5 & -0.9 \\ 0 & -0.5 & 0 \end{bmatrix} \quad \mathbf{B} = \begin{bmatrix} 0 & 0 & 0 \\ 0 & 1 & 0 \\ 0 & 0 & 0 \end{bmatrix} \quad \xi = 2.1$$

**Table 1.** Different dynamical behaviors with the same template but with different input and initial state. The time evolution of one cell from the second row, logarithm of power spectrum of the same cell and the 2D trajectory of the same cell and the neighbor are shown.



**Table 2.** Effect of one pixel perturbation. The circle denotes the location of the perturbation.

Inputs		Outputs		Template 8:		
				$\mathbf{A} = \begin{bmatrix} 0 & 0 & 0 \\ 1 & 0.5 & -1 \\ 0 & -0.5 & 0 \end{bmatrix}$	$\mathbf{B} = \begin{bmatrix} 0 & 0 & 0 \\ 0 & 1.3 & 0 \\ 0 & 0 & 0 \end{bmatrix}$	$\zeta = 0$

## 6 Simulation time vs. real-time measurements

A sophisticated simulation of chaotic systems takes several minutes (or even hours), especially when the dimension of the system is high. Using the new programmable ACE4K test bed it is possible to speed up the analysis process of the chaotic system by at least four orders of magnitude.

## 7 Conclusion

Both the simulations and the real-time experiments with the ACE4k test bed showed that if we add a single nonzero element  $r$  to a CCD-like antisymmetric template, the behavior of the system is significantly changes, complex dynamics occurs and characteristic patterns are formed. At certain parameter settings – especially when the self-feedback  $p$  is high – the output pattern showed a unique chaotic pattern. The layout of the  $r$ - $p$  parameter space showed characteristic structure. We expect that future works discover additional interesting and useful properties of this template class and helps to understand more the complex dynamics. It would also lead to a new class of analogic spatial-temporal algorithms for the dynamic detection of exotic and complex events.

## Acknowledgements

This research was supported by the ONR Grant No.: N00014-00 1 0429 and the Hungarian National Foundation (OTKA) Grant No.: T O26 555.

## References

1. G. Liñan, S. Espejo, R. Domínguez-Castro, A. Rodríguez-Vázquez, “The CNNUC3: An Analog I/O 64x64 CNN Universal Machine Chip Prototype with 7-Bit Analog Accuracy”, Proceedings of IEEE Int. Workshop on Cellular Neural Networks and Their Applications, (CNNA'2000), pp. 201-206, Catania, 0-7803-6344-2, 2000
2. L.O. Chua and L. Yang, “Cellular Neural Networks: Theory”, IEEE Trans. on Circuits and Systems, Vol.35. pp. 1257-1272, 1988.
3. L.O. Chua and L. Yang, “Cellular neural networks: Applications”, IEEE Trans. on Circuits and Systems, Vol.35. pp. 1273-1290, 1988.
4. L.O. Chua and T. Roska, “The CNN paradigm”, IEEE Trans. on Circuits and Systems I: Fundamental Theory and Applications, Vol.40, No. 3, pp. 147-156, 1993.

5. T. Roska and L.O. Chua, The CNN universal machine: an analogic array computer, IEEE Trans. on Circuits and Systems II: Analog and Digital Signal Processing Vol. 40, No. 3, pp. 163-173, 1993.
6. A. Rodriguez-Vázquez, S. Espejo, R. Dominguez-Castro, J.L. Huertas, and E.Sánchez-Sinencio, “Current-Mode Techniques for the Implementation of Continuous- and Discrete-Time Cellular Neural Networks”, IEEE Trans. on Circuits and Systems II: Analog and Digital Signal Processing, Vol.40. No.3. pp. 132-146, 1993
7. F. Zou and J.A. Nossek, “Stability of cellular neural networks with opposite sign templates”, IEEE Trans. on Circuits and Systems, (CAS), Vol. 38. pp. 675-677, 1991
8. P. Thiran, G. Setti, and M. Hasler, “An approach to information propagation in 1-D cellular neural networks—Part I: Local diffusion”, IEEE Trans. Circuits Systems I, Vol.45, No.8, pp. 777–789, 1998.
9. G. Setti, P. Thiran, and C. Serpico, “An approach to information propagation in 1-D cellular neural networks—Part II: Global Propagation”, IEEE Trans. Circuits Systems I, Vol.45, No.8, pp. 790–811, 1998.
10. P. Thiran, K. R. Crouse, L. O. Chua, and M. Hasler, “Pattern formation properties of autonomous cellular neural networks,” IEEE Trans. Circuits Systems I, vol. 42, pp. 757–776, Oct. 1995.
11. F. Zou, J.A. Nossek, “Bifurcation and Chaos in Cellular Neural Networks”, IEEE Trans. on Circuits and Systems I: Fundamental Theory and Applications, (CAS-I), Vol.40, No.3, pp.166-173, 1993
12. M. Biey. M. Gilli, and P. Checco, “Complex Dynamic Phenomena in Space-Invariant Cellular Neural Networks”, IEEE Trans. on Circuits and Systems I: Special Issue, March 2000 (in print).
13. G. Manganaro, P. Arena, L. Fortuna “Cellular Neural Networks: Chaos, Complexity and VLSI Processing”, Springer Verlag, New York; ISBN: 3540652027, 1999
14. L. O. Chua and T. Roska, “Stability of a Class of Nonreciprocal Cellular Neural Networks”, IEEE Trans. on Circuits and Systems, Vol.37.pp. 1520-1527, 1990
15. I. Petrás, T. Roska, L.O. Chua, “New spatial-temporal patterns and the first programmable on-chip bifurcation test-bed”, Research report of the Analogic (Dual) and Neural Computing Systems Laboratory, (DNS-6-2001), Budapest MTA SZTAKI, 2001